

# A TWO-FLUID APPROXIMATION FOR CALCULATING THE COSMIC MICROWAVE BACKGROUND ANISOTROPIES

Uroš Seljak<sup>1</sup>

Department of Physics, MIT, Cambridge, MA 02139 USA

## ABSTRACT

We present a simple, yet accurate approximation for calculating the cosmic microwave background anisotropy power spectrum in adiabatic models. It consists of solving for the evolution of a two-fluid model until the epoch of recombination and then integrating over the sources to obtain the CMB anisotropy power spectrum. The approximation is useful both for a physical understanding of CMB anisotropies, as well as for a quantitative analysis of cosmological models. Comparison with exact calculations shows that the accuracy is typically better than 20 percent over a large range of angles and cosmological models, including those with curvature and cosmological constant. Using this approximation we investigate the dependence of the CMB anisotropies on the cosmological parameters. We identify six dimensionless parameters that uniquely determine the anisotropy power spectrum within our approximation. CMB experiments on different angular scales could in principle provide information on all these parameters. In particular, mapping of the Doppler peaks would allow an independent determination of baryon mass density, matter mass density and Hubble constant.

*Subject headings:* cosmology-cosmic microwave background

## 1. Introduction

---

<sup>1</sup>Also Department of Physics, University of Ljubljana, Jadranska 19, 61000 Ljubljana, Slovenia

Observations of fluctuations in cosmic microwave background (CMB) can provide important constraints on cosmological models. Large angular scale ( $> 10^0$ ) observations probe the initial conditions, in particular the amplitude and the slope of primordial power spectrum (Smoot et al. 1992; Górski et al. 1994; Wright et al. 1994). These scales could also provide information on the geometry and the matter content of the universe (Kofman & Starobinsky 1985; Kamionkowski & Spergel 1994; Sugiyama & Silk 1994). However, theoretical interpretation of measurements on these scales is complicated by cosmic variance and this intrinsically limits the accuracy with which these parameters can be estimated using large angular scale measurements alone. While small scale measurements suffer less from cosmic variance, their interpretation is complicated by the microphysics during recombination and/or reionization. Theoretical models often give wildly different predictions for the anisotropy power spectra when the parameter values are only slightly changed, while some combinations of parameters seem to provide nearly identical spectra (e.g. Bond et al. 1994). The purpose of this Letter is to clarify which combinations of physical parameters affect the CMB fluctuations and what are the physical processes that lead to these fluctuations. Our two-fluid model for adiabatic fluctuations, presented in §2, generalizes previous theoretical approximations that investigated CMB fluctuations in the limiting cases of large and small angles (Sachs & Wolfe 1966; Jørgensen et al. 1994). The model is accurate enough that it can be used for a quantitative analysis of various models, yet it is also simple enough that it can clearly separate between different physical processes that affect the CMB fluctuations. In §3 we use this model to identify the physical parameters that can be determined using CMB measurements over a large angular range, extending previous studies that were limited to a smaller range of angles and/or parameters (Bond et al. 1994; Kamionkowski, Spergel & Sugiyama 1994; Górski & Stompor 1994; Sugiyama & Silk 1994; Muciaccia et al. 1993). In §4 we present the conclusions.

## 2. Method

In this section we present a method for computing the CMB anisotropies that is a generalization of analytic methods first introduced by Sachs & Wolfe (1966) and is based on the line-of-sight integration along the photon past light cone. We will assume that the photons and baryons are tightly coupled prior to recombination, which will allow a simple two-fluid description of perturbations (Peebles & Yu 1970). Our analysis will be restricted to the linear perturbation theory of adiabatic perturbations and we will neglect any possible tensor contributions. Different theoretical models will be compared using angular power spectrum of CMB anisotropies,  $C_l = \langle |a_{lm}|^2 \rangle$ , where  $a_{lm}$  is the multipole of temperature

anisotropy  $\Delta(\vec{n}) = \sum_{l,m} a_{lm} Y_{lm}(\vec{n})$  and  $Y_{lm}(\vec{n})$  is the spherical harmonic. Expected CMB anisotropy for a given experiment can be calculated from  $\langle \Delta^2 \rangle = \sum_{l \geq 2} (2l+1) W_l C_l / 4\pi$ , where  $W_l$  is the experiment window function.

The temperature fluctuation  $\Delta(\vec{n})$  in the direction  $\vec{n}$  can be expressed as a line-of-sight integral,

$$\Delta(\vec{n}) = \int_0^{\tau_0} [\dot{\mu}(\phi + \frac{\delta_\gamma}{4} + \vec{n} \cdot \vec{v}_b) + 2\dot{\phi}] e^{-\mu} d\tau. \quad (1)$$

Here  $\tau$  is the conformal time with the value  $\tau_0$  today,  $\phi$  is the gravitational potential,  $\delta_\gamma$  is the photon density perturbation and  $\vec{v}_b$  is the electron velocity. We introduced the Thomson opacity along the past light cone  $\mu(\tau) = \int_\tau^{\tau_0} \dot{\mu}(\tau') d\tau'$  with  $\dot{\mu} = a x_e n_e \sigma_T$ , where  $a$  is the expansion factor,  $x_e$  the ionization fraction,  $n_e$  the electron number density and  $\sigma_T$  the Thomson cross section. The above expression is written in the gauge invariant formalism (Kodama & Sasaki 1984). We neglected the anisotropic stress contribution and the unobservable monopole contribution arising from the local gravitational potential. In the limit of infinitely thin LSS the function  $\dot{\mu} e^{-\mu}$  approaches to a Dirac delta-function  $\delta(\tau - \tau_{rec})$ , where  $\tau_{rec}$  denotes the conformal time at recombination. Equation 1 then reduces to (Kodama & Sasaki 1984)

$$\Delta(\vec{n}) = \phi(\tau_{rec}) + \frac{\delta_\gamma(\tau_{rec})}{4} + \vec{n} \cdot \vec{v}_b(\tau_{rec}) + 2 \int_{\tau_{rec}}^{\tau_0} \dot{\phi}(\tau) d\tau. \quad (2)$$

The velocity term in equation 2 can be rewritten using the linear theory approximation  $\vec{v}_b = \vec{\nabla} \psi_b$  into  $\vec{n} \cdot \vec{v}_b = \partial \psi_b / \partial r$ , where  $r$  is the radial coordinate. We may decompose the sources in equation 2 into an orthonormal spherical basis set with Fourier amplitudes  $\phi(k)$ ,  $\delta_\gamma(k)$  and  $v_b(k)$ , where  $v_b(k) = i\psi_b(k)/k$ . After the angular and ensemble averaging we obtain the following expression for the multipole moments (Kodama & Sasaki 1984),

$$\begin{aligned} C_l &= 4\pi \int_0^\infty k^2 P(k) T(k) D_l^2 dk \\ D_l &= (\phi + \frac{\delta_\gamma}{4}) j_l(k\tau_0 - k\tau_{rec}) + v j'_l(k\tau_0 - k\tau_{rec}) + 2 \int_{\tau_{rec}}^{\tau_0} d\tau j_l(k\tau_0 - k\tau) \dot{F}(\tau), \end{aligned} \quad (3)$$

where  $j_l$  is the spherical Bessel functions and  $j'_l$  its derivative. All the perturbed quantities are evaluated in  $k$ -space at  $\tau_{rec}$ .  $P(k)$  denotes the primordial power spectrum of potential  $\phi$ , usually expressed as a power law  $P(k) \propto k^{n-4}$ . For later purpose we introduced the function  $T(k)$ , which incorporates the damping effects. In the case of a non-flat universe the functions  $j_l$  need to be substituted by their appropriate generalizations. This is unimportant for  $l > \Omega_0^{-1} |1 - \Omega_0|^{1/2}$  and the results presented here will be valid for non-flat universes, provided that the relation between angles and physical sizes is expressed using angular size distances. Last term in equation 3 gives the so-called integrated Sachs-Wolfe

(ISW) contribution. The time dependence of the potential is denoted with  $\dot{F}(\tau)$ , where  $F(\tau) = \phi(\tau)/\phi(\tau_0)$ . This term vanishes in a flat, matter dominated  $\Omega_m = 1$  universe, but is present in the case of a vacuum energy dominated universe (Kofman & Starobinsky 1985), curvature dominated universe (Kamionkowski & Spergel 1994) or when the universe is in transition epoch from being radiation to being matter dominated (Kodama & Sasaki 1986).

To calculate the anisotropy power spectrum we need to evaluate the source contributions in equation 3 at the epoch of recombination. The photon evolution equations in  $k$ -space are given by (Ma & Bertschinger 1994; Wilson & Silk 1981; Bond & Efstathiou 1984)

$$\dot{\delta}_\gamma = -\frac{4}{3}kv_\gamma + 4\dot{\phi}, \quad \dot{v}_\gamma = \frac{k\delta_\gamma}{4} + \dot{\mu}(v_b - v_\gamma) + k\phi. \quad (4)$$

We also need the evolution equations for baryon and CDM perturbations,

$$\begin{aligned} \dot{\delta}_b &= -kv_b + 3\dot{\phi}, & \dot{v}_b &= -\frac{\dot{a}}{a}v_b + \frac{4\bar{\rho}_\gamma}{3\bar{\rho}_b}\dot{\mu}(v_\gamma - v_b) + k\phi \\ \dot{\delta}_c &= -kv_c + 3\dot{\phi}, & \dot{v}_c &= -\frac{\dot{a}}{a}v_c + k\phi, \end{aligned} \quad (5)$$

where  $\bar{\rho}_b$  and  $\bar{\rho}_\gamma$  are the baryon and photon mean densities, respectively.

The energy and momentum constraint equations give the equations for  $\phi$  and  $\dot{\phi}$ ,

$$\phi = -\frac{4\pi Ga^2}{k^2}(\rho + \frac{3\dot{a}f}{ak}), \quad \dot{\phi} = -\frac{\dot{a}}{a}\phi + \frac{4\pi Ga^2f}{k}, \quad (6)$$

where  $\rho = (\bar{\rho}_\gamma + \bar{\rho}_\nu)\delta_\gamma + \bar{\rho}_b\delta_b + \bar{\rho}_c\delta_c$  and  $f = \frac{4}{3}(\bar{\rho}_\gamma + \bar{\rho}_\nu)v_\gamma + \bar{\rho}_b v_b + \bar{\rho}_c v_c$ . Here  $\bar{\rho}_\nu$  and  $\bar{\rho}_c$  are the neutrino and CDM mean densities, respectively. We replaced neutrino density and velocity perturbations with the corresponding photon perturbations. This becomes invalid on small scales due to the free-streaming of neutrinos, but does not affect significantly the final results. We also neglected the anisotropic shear and the possible curvature terms.

The above equations are supplemented by the Friedmann equation, which at early times (when a possible cosmological constant or curvature term can be neglected) is given by

$$(\frac{\dot{a}}{a})^2 = \frac{8\pi Ga^2}{3}(\bar{\rho}_\gamma + \bar{\rho}_\nu + \bar{\rho}_b + \bar{\rho}_c). \quad (7)$$

The solution to this equation is

$$y \equiv \frac{a}{a_{eq}} = (\alpha x)^2 + 2\alpha x, \quad x = \left(\frac{\Omega_m}{a_{rec}}\right)^{1/2} \frac{H_0\tau}{2} \equiv \frac{\tau}{\tau_r}, \quad (8)$$

where  $a_{eq} = (\bar{\rho}_\gamma + \bar{\rho}_\nu)/(\bar{\rho}_b + \bar{\rho}_c) \approx 4.2 \times 10^{-5}\Omega_m^{-1}h^{-2}$  (assuming three flavors of massless neutrinos),  $a_{rec}^{-1} \approx 1100$  for the standard recombination,  $\alpha^2 \equiv a_{rec}/a_{eq}$ ,  $\Omega_m = \Omega_b + \Omega_c$  is

the value of matter density today in units of critical density and  $h$  is the value of Hubble constant today in units of 100km/s/Mpc.

We will now assume the tight coupling limit  $\mu \gg 1$ , which is a good approximation on scales larger than the Silk damping scale (Silk 1968, Peebles & Yu 1970). In this case the photons and baryons are coupled into a single fluid with  $\delta_b = \frac{3}{4}\delta_\gamma$  and  $v_b = v_\gamma$ . The above equations rewritten in terms of dimensionless time  $x$  and dimensionless wavevector  $\kappa = k\tau_r$  become

$$\begin{aligned} \dot{\delta}_c &= -\kappa v_c + 3\dot{\phi}, & \dot{v}_c &= -\eta v_c + \kappa\phi \\ \dot{\delta}_\gamma &= -\frac{4}{3}\kappa v_\gamma + 4\dot{\phi}, & \dot{v}_\gamma &= \left(\frac{4}{3} + y_b\right)^{-1} \left[ -\eta y_b v_\gamma + \frac{\kappa\delta_\gamma}{3} + \kappa\phi\left(\frac{4}{3} + y_b\right) \right] \\ \phi &= -\frac{3}{2}(\eta/\kappa)^2(\delta + 3\eta v/\kappa), & \dot{\phi} &= -\eta\phi + \frac{3\eta^2 v}{2\kappa} \\ \delta &= \frac{\delta_\gamma[1+\frac{3}{4}(y-y_c)]+y_c\delta_c}{1+y}, & v &= \frac{v_\gamma(\frac{4}{3}+y-y_c)+y_c v_c}{1+y}, \end{aligned} \quad (9)$$

where the derivatives are taken with respect to  $x$ ,  $y_b \equiv \frac{\bar{\rho}_b}{\bar{\rho}_\gamma} = [1 + \frac{3\times 7}{8}(\frac{4}{11})^{4/3}] \frac{\Omega_b}{\Omega_m} y = 1.68 \frac{\Omega_b}{\Omega_m} y$ ,  $y_c = \frac{\Omega_c}{\Omega_m} y = (1 - \frac{\Omega_b}{\Omega_m}/1.68)y$  and  $\eta = 2\alpha(\alpha x + 1)/(\alpha^2 x^2 + 2\alpha x)$ . Equations 9 are a coupled system of 4 first order differential equations.<sup>2</sup> The appropriate initial conditions at  $x \ll 1$  (when the universe is radiation dominated) and  $\kappa\eta \ll 1$  (when the mode is larger than the Hubble sphere radius) are

$$\begin{aligned} \phi &= 1, & \delta_\gamma &= -2\phi(1 + \frac{3y}{16}), & \delta_c &= \frac{3}{4}\delta_\gamma \\ v_\gamma &= v_c = -\frac{\kappa}{\eta} \left[ \frac{\delta_\gamma}{4} + \frac{2\kappa^2(1+y)\phi}{9\eta^2(\frac{4}{3}+y)} \right]. \end{aligned} \quad (10)$$

The above equations need to be evolved until  $x_{rec} = [(\alpha^2 + 1)^{1/2} - 1]/\alpha$ . The temperature anisotropy expressed with the dimensionless variables is given by

$$C_l = 4\pi A \int_0^\infty \kappa^n T(\kappa) d\ln\kappa \left[ \left( \phi + \frac{\delta_\gamma}{4} + 2\Delta\phi \right) j_l(\kappa x_0) + v_\gamma j'_l(\kappa x_0) \right]^2, \quad (11)$$

where  $x_0$  is the angular distance to the LSS in units of  $\tau_r$  and we assumed  $P(k) = Ak^{-3}\kappa^{n-1}$ . The term  $\Delta\phi = [2 - 8/y(x_{rec}) + 16x_{rec}/y^3(x_{rec})]/10y(x_{rec})$  arises from the ISW effect due to the potential varying with time during the transition period from the radiation dominated

---

<sup>2</sup> In actual numerical implementation of these equations we find that for a stable numerical integration it is better to compute  $\phi$  using its time evolution in equation 9, rather than computing it from the sources.

to the matter dominated universe (Kodama & Sasaki 1986). For simplicity we dropped the ISW contribution from possible curvature or cosmological constant, which is only important at the lowest values of  $l$  ( $l < 10$ ).

The damping transfer function  $T(\kappa)$  is approximately unity for low values of  $l$  ( $l < 200$ ), but gradually decreases afterwards. Its main contributions come from the Silk damping and from the finite width of LSS. The first effect can be calculated analytically by expanding equations 4 and 5 to second order in  $\dot{\mu}$  and neglecting the effects of gravity and expansion. In the matter-dominated era one obtains  $T(\kappa) \propto \exp(-2\kappa^2 x_s^2)$  (Fugukita et al. 1990), where  $x_s$  is the Silk damping scale in units of  $\tau_r$ ,  $x_s = 0.6\Omega_m^{1/4}\Omega_b^{-1/2}a_{rec}^{3/4}h^{-1/2}$ . Second effect can be analytically estimated by performing the line-of-sight integral in equation 1 in the limit where the sources are slowly changing over the timescale on which the visibility function  $\dot{\mu}e^{-\mu}$  is non-negligible (Jørgensen et al. 1994). Visibility function can be approximated as a gaussian  $(2\pi\sigma^2 x_{rec}^2)^{-1/2} \exp[-(x - x_{rec})^2/2(\sigma x_{rec})^2]$ , where for standard recombination  $\sigma \approx 0.03$ .<sup>3</sup> In the limit  $\kappa_0 x_0 \gg l$  (where  $\kappa_0$  is the wavevector which gives the dominant contribution to  $C_l$ ), we obtain the damping factor  $\exp(-\kappa^2 \sigma^2 x_{rec}^2)$ . Therefore, the damping effects can be written as

$$T(\kappa) \approx e^{-\kappa^2(2x_s^2 + \sigma^2 x_{rec}^2)}. \quad (12)$$

This works reasonably well for the standard ionization history. Note however that if the limit  $\kappa_0 x_0 \gg l$  is not satisfied, then the damping due to the finite thickness of LSS is not exponential, but is proportional to  $\kappa^{-1}$ . This will be the case, for example, in reionized models.

Equations 9-12 are all needed to evaluate the temperature fluctuations. Although equations 9 cannot be solved analytically in general, they have analytic solutions in the limits of small and large  $\kappa$ . In the first limit where the modes are larger than the Hubble sphere radius the amplitude of perturbations at a given time is a constant (figure 1). This gives the standard Sachs-Wolfe expression for CMB fluctuations, as can be verified by evolving the initial conditions in equations 10 into the matter-dominated era and neglecting the velocity term in equation 11. In the second limit (large  $\kappa$ ) the equations can be solved using the WKB approximation and the solution is given by the acoustic oscillations of photon-baryon plasma (Jørgensen et al. 1994, Padmanabhan 1993). In the intermediate regime, which is of main interest for us, the equations need to be solved numerically, but the physics can be well understood by the two limits above. As shown in figure 1, equations 9 give an excellent approximation to the exact results over a large range of wavevector  $\kappa$ .

---

<sup>3</sup>Both  $\sigma$  and  $a_{rec}$  are weakly dependent on cosmological parameters. Moreover, the ISW visibility function differs from the Thomson scattering visibility function, which leads to a different damping of ISW term. Both effects will be neglected here.

Although the above system of equations is particularly useful for the standard recombination scenarios, one can also use it to calculate anisotropy power spectrum in reionized models. As one can see from equation 1, the primary fluctuations will be suppressed by a factor  $\exp[-\mu(x_{rec})]$ , where  $\mu(x_{rec})$  is Thomson opacity at recombination. In addition, there will be secondary fluctuations generated at the new last-scattering surface, which can be calculated using the same method as above, except that one needs to replace  $v_\gamma$  with  $v_c$  in the regime where the Compton drag is negligible. Since the modes larger than the Hubble sphere radius at the new LSS do not evolve in the matter-dominated regime this simply regenerates the Sachs-Wolfe expression for low values of  $l$ . On smaller scales the thick new LSS damps the secondary fluctuations and in many scenarios these become negligible (although on arcminute scales the second-order terms may become important, Vishniac 1987). Provided that one is interested in degree angular scales, then the effect of reionization is to suppress the fluctuation power spectrum relative to the large scales by a factor of  $\exp[-2\mu(x_{rec})]$ .

### 3. Results

The comparison between our approximation and the exact solutions of perturbed Boltzmann equation (Seljak & Bertschinger 1994; Seljak 1994) is presented in figure 2 for several cosmological models. All of the multipole moments are normalized relative to  $C_{10}$ , which is approximately fixed by the COBE experiment and where the curvature effects and ISW effects due to  $\Omega_m \neq 1$  can be neglected. One can see that the agreement is excellent over a large range of  $l$ . The deviations at large  $l$  arise because of improper treatment of damping effects, while the deviations at small  $l$  can be attributed to the neglection of neutrino anisotropic shear. Another effect that introduces small deviations is the dependence of  $a_{rec}$  on cosmological parameters, which slightly offsets the position of the peaks. Nevertheless, our approximation correctly predicts the positions and amplitudes of Doppler peaks (also called acoustic or Sakharov oscillations) with a 20 % accuracy over most of parameter range.

Given the high accuracy of our model we may now investigate how the anisotropy power spectrum depends on the cosmological model. Our goal is to identify the parameters that can be determined using the CMB measurements and to give a physical understanding of how they affect the anisotropies. In equations 9 the free parameters are  $\alpha = 21.5\Omega_m^{1/2}h$  and  $\frac{\Omega_b}{\Omega_m}$ . We can replace them with physically more relevant parameters  $\Omega_m h^2 = (\alpha/21.5)^2$  and  $\Omega_b h^2 = (\alpha/21.5)^2 \frac{\Omega_b}{\Omega_m}$ . In addition to these two we have the parameters  $\mu(x_{rec})$ ,  $n$ ,  $x_0$

and  $x_s$ . These six parameters will uniquely determine all the CMB power spectra within our approximation. Of the parameters above,  $n$ ,  $\mu(x_{rec})$  and  $x_s$  all suppress the power on small scales relative to large scales (for  $n < 1$ ). The suppression is different in the three cases, being proportional to  $\kappa^{n-1}$  (neglecting the possible tensor contribution),  $\exp[-\mu(x_{rec})]$  and  $\exp(-2\kappa^2 x_s^2)$ , respectively. This, in principle, allows to separate the different suppression effects and to determine the three parameters separately (but see Bond et al. 1994). Note that these parameters do not change the positions of the Doppler peaks, only their amplitude. Since the effects of these parameters are physically transparent, we will restrict in the following to the case of  $n = 1$  and  $\mu(x_{rec}) = 0$ . Moreover, Silk damping is important only for large values of  $l$  and it can be neglected if one concentrates on the first few Doppler peaks. We are thus left with  $x_0$ ,  $\Omega_m h^2$  and  $\Omega_b h^2$ , which uniquely determine positions of the Doppler peaks.

Position of the first Doppler peak is determined by the angular size of the Hubble sphere radius at decoupling, which, expressed in terms of our variables is given by  $(1 + \alpha^{-2})^{1/2} x_0$ . Since  $\alpha \gg 1$  for typical values of  $\Omega_m h^2$ , position of the first Doppler peak mainly depends on  $x_0$ . Assuming  $x_{rec} \ll x_0$  we have  $x_0 = (\Omega_m a_{rec})^{-1/2}$  for the model with negligible cosmological constant and  $x_0 = \Omega_m^{0.09} a_{rec}^{-1/2}$  for the model with negligible curvature. The latter result shows that the first Doppler peak only weakly depends on  $\Omega_\lambda = 1 - \Omega_m$ . This is because the angular size distance at large redshifts scales with  $\Omega_m$  in approximately the same way as does the Hubble sphere radius at decoupling (Vittorio & Silk 1985; Górski & Stompor 1994). This is, however, not true in general and the position of the first Doppler peak depends on  $\Omega_m$  and  $\Omega_\lambda$  when both curvature and cosmological constant are important. The value of  $l$  at which the maximum of the first Doppler peak lies is given approximately by  $6x_0$ . Figure 3a compares  $C_l$ 's of curvature and cosmological constant dominated models with those of  $\Omega_m = 1$  model at fixed values of  $\Omega_m h^2$  and  $\Omega_b h^2$ . One can see that the position of the first Doppler peak can accurately determine  $\Omega_m$  in curvature dominated universe (Kamionkowski, Spergel & Sugiyama 1994), but cannot precisely determine  $\Omega_m$  in cosmological constant dominated universe (Bond et al. 1994; Górski & Stompor 1994). However, even in this model the positions of secondary Doppler peaks are already significantly displaced relative to each other when  $\Omega_m$  changes from 0.25 to 1. This would thus allow independent determination of  $\Omega_m$  even in cosmological constant dominated universe, once  $\Omega_m h^2$  and  $\Omega_b h^2$  are known (see below).

The dependence of the Doppler peak positions and amplitudes on  $\Omega_b h^2$  and  $\Omega_m h^2$  is more complicated, since both parameters appear in the evolution equations 9 and change the properties of acoustic oscillations. Moreover, the two parameters enter into the equations differently and have different physical effects:  $\Omega_b h^2$  is related to the properties of photon-baryon plasma and determines its effective sound velocity at recombination, whereas

$\Omega_m h^2$  is related to the time evolution of the expansion factor, since it determines the epoch of matter-radiation equality. This means that one cannot expect the anisotropy spectra to remain invariant under a certain combination of the two parameters and both  $\Omega_b h^2$  and  $\Omega_m h^2$  are required for a complete description of the Doppler peaks. Figures 3b and 3c show how the Doppler peaks change when one of the two parameters is changing while the other is held fixed. If one concentrates on the first Doppler peak then it is not possible to determine the two parameters simultaneously, since both increasing  $\Omega_b h^2$  and decreasing  $\Omega_m h^2$  lead to an increase in the first Doppler peak. The physical mechanisms that lead to this are different: while an increase in  $\Omega_b h^2$  increases the amplitude of the first wave in  $v_\gamma$  and  $\phi + \delta_\gamma/4$  (fig. 1), a decrease in  $\Omega_m h^2$  also leads to an increased ISW contribution. Once the secondary peaks are observed as well, then different effects of the two parameters become significant and allow one to determine the two parameters simultaneously (figs. 3 b,c,d). Figure 3d shows how changing  $\Omega_m h^2$  at a fixed value of  $\frac{\Omega_b}{\Omega_m}$  affects the multipole moments. Again, since the epoch of matter-radiation equality is changing with  $\Omega_m h^2$ , one does not expect the multipole moments to remain unchanged and both our approximation and exact calculations confirm this. Therefore, changing  $h$  at a fixed  $\Omega_b$  and  $\Omega_m$  changes the anisotropy power spectrum, contrary to some recent claims (Bond et al. 1994; Górski & Stompor 1994).

#### 4. Discussion

The approximation for calculating anisotropy power spectrum presented here is a generalization of the Sachs-Wolfe approximation, which itself is only valid on scales larger than the Hubble sphere radius at recombination. By modelling the cosmological perturbations as a two-component fluid plasma we extended this approach to all scales. The approximation is useful both for developing the physical understanding of processes that affect CMB fluctuations, as well as for a quantitative prediction of multipole moments for various cosmological models. The main approximations used in our model are a two-fluid approximation, neglection of anisotropic shear, a simplified treatment of Thomson scattering effects, neglection of curvature effects and neglection of vector and tensor contributions. None of these assumptions is essential for the method and one can generalize the approach presented here to obtain exact results (Seljak 1994). This will lead to a computationally more demanding system of equations, but the main physical effects that lead to the creation of Doppler peaks will still be determined by the equations presented in this Letter.

By rewriting the equations in their dimensionless form we identified all the dimensionless parameters that affect the anisotropy power spectra. Measurements of CMB fluctuations

can only determine these parameters. For example, neutrinos enter into our equations indirectly through the Friedmann equation 7 and through the energy-momentum constraint equations 6. The presence of a massive neutrino only weakly changes these equations and the resultant multipole moments are almost indistinguishable from the ones with the massless neutrino. Therefore, the question of whether neutrino has a mass has little hope to be answered using the CMB measurements.

The most interesting aspect of the CMB power spectra is the peculiar pattern of the Doppler peaks, which allows a simultaneous determination of  $\Omega_b h^2$  and  $\Omega_m h^2$ . This would provide an independent test of nucleosynthesis prediction of  $\Omega_b h^2$  (e.g. Walker et al. 1991) and would also constrain the parameter space on  $\Omega_m$  and  $h$ . In addition, the position of the first Doppler peak determines  $\Omega_m$  in curvature dominated model. In cosmological constant dominated model the position of the first Doppler peak does not allow one to determine  $\Omega_m$  accurately, but positions of secondary Doppler peaks could be used to constrain  $\Omega_m$  (although for accurate determination exact calculations should be used in this case). Another way to break the degeneracy between  $\Omega_m$ ,  $\Omega_b$  and  $h$  is to determine the Silk damping scale  $x_s$ , which depends only on these three parameters and cannot be expressed as a combination of  $\Omega_b h^2$  and  $\Omega_m h^2$ . This would require a separation of Silk damping from the damping due to the finite thickness of LSS in reionized models and from the  $n < 1$  suppression of small scales relative to large scales (including the possible tensor contribution). This is possible, because the three effects suppress the small scale power differently. Thus, a combination of CMB measurements over a large range of angles could be used to separately determine the baryon mass density, matter mass density and the Hubble constant value.

I would like to thank Ed Bertschinger for useful discussions. This work was supported by grants NSF AST90-01762 and NASA NAGW-2807.

## REFERENCES

Bond, J. R., & Efstathiou, G. 1984, ApJ, 285, L45

Bond, J. R., Crittenden, R., Davis, R. L., Efstathiou, G., & Steinhard, P. J. 1994, Phys.Rev.Lett, to be published

Fugukita, M., Sugiyama, N., & Unemura, M. 1990, ApJ, 358, 28

Górski, K. M. et al. 1994, ApJ, to be published

Górski, K. M., & Stompor, K. M. 1994, ApJ, 422, L41

Jørgensen, H.E., Kotok, E., Naselsky, P., & Novikov, I. 1994, A&A, to be published

Kamionkowski, M. & Spergel, D. N. 1994, ApJ, to be published

Kamionkowski, M., Spergel, D. N., & Sugiyama, N. 1994, ApJ, 426, L57

Kodama, H., & Sasaki, M. 1984, Prog. Theor. Phys. Suppl. 78, 1

Kodama, H., & Sasaki, M. 1986, Int. J. Mod. Phys. A1, 265

Kofman, L., & Starobinsky, A. 1985, Sov. Astron. Lett., 11, 271

Ma, C. P., & Bertschinger, E. 1994, ApJ, to be published

Muciaccia, P. F., Mei, S., De Gasperis, G., & Vittorio, N. 1993, ApJ, 410, L61

Padmanabhan, T. 1993, Structure Formation in the Universe, Cambridge: Cambridge University Press

Peebles, P. J. E., & Yu, I. T. 1970, ApJ, 162, 815

Sachs, R. K. & Wolfe, A. M. 1966, ApJ, 147, 73

Seljak, U. 1994, in preparation

Seljak, U., & Bertschinger, E. 1994, to appear in "Present and Future of the Cosmic Microwave Background", eds. J. L. Sanz, E. Martinez-Gonzalez, & L. Cayon (in press)

Silk, J. 1968, ApJ, 151, 459

Smoot, G. F. et al. 1993, ApJ, 396, L1

Sugiyama, N. & Silk, J. 1994, Phys.Rev.Lett, in press

Vishniac, E. T. 1987, ApJ, 322, 597

Vittorio, N., & Silk, J. 1985, ApJ, 297, L1

Walker, T. P., Steigman, G., Schramm, D. N., Olive, K. A., & Kang, H. 1991, ApJ, 376, 51

Wilson, M. L., & Silk, J. 1981, ApJ, 243, 14

Wright, E. L. et al. 1994, ApJ, to be published

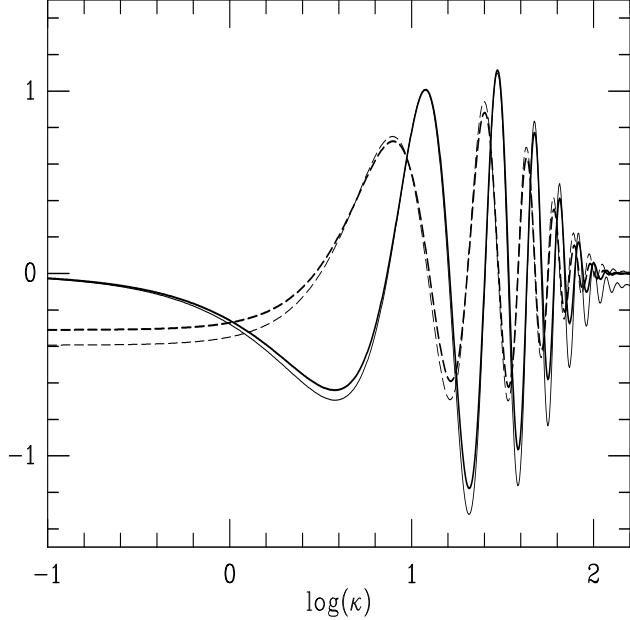


Fig. 1.— Comparison between our approximation (thick lines) and exact solution (thin lines) for  $v_\gamma$  (solid lines) and  $\phi + \delta_\gamma/4$  (dashed lines) as a function of  $\kappa$ . Silk damping has been included according to the expression in the text. Parameter values are  $\Omega_b = 0.05$ ,  $h = 0.5$  and  $\Omega_m = 1$ .

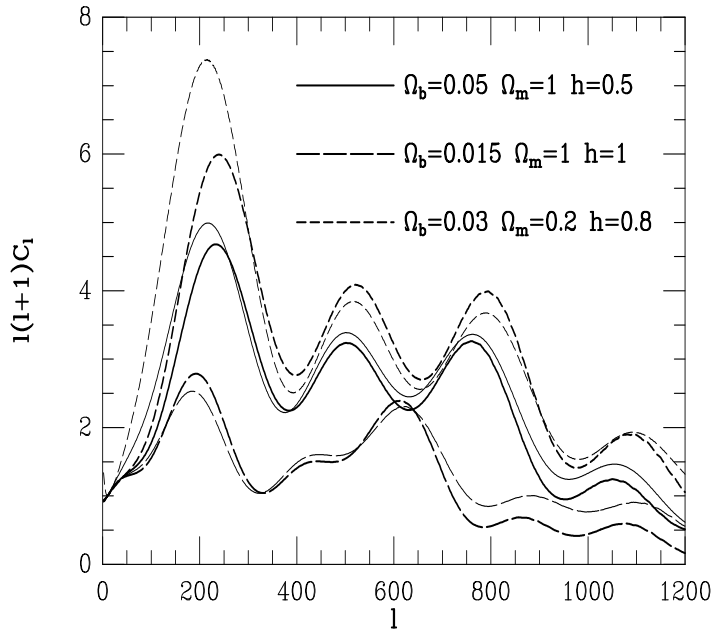


Fig. 2.— Comparison of anisotropy power spectra between our approximation (thick lines) and exact solution (thin lines) as a function of multipole moment  $l$  for several different cosmological models. The spectra in all figures are normalized relative to  $C_{10}$ .

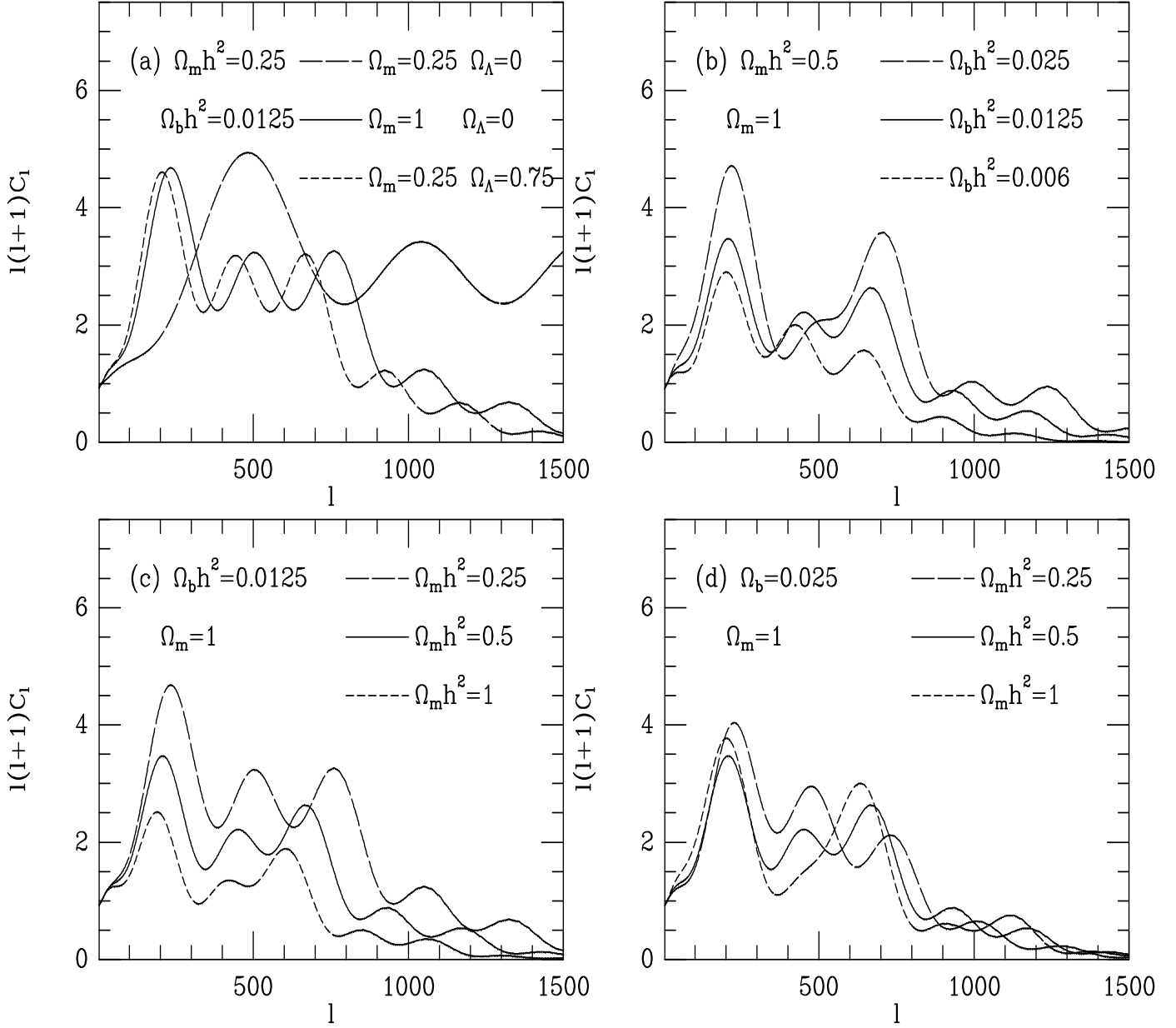


Fig. 3.— Anisotropy power spectra as a function of multipole moment  $l$  for different cosmological models. In (a) curvature and cosmological constant dominated models with  $\Omega_m = 0.25$  are compared to  $\Omega_m = 1$  model. In (b)  $\Omega_m h^2$  is fixed at 0.5 and  $\Omega_b h^2$  is varying, whereas in (c)  $\Omega_b h^2$  is fixed at the nucleosynthesis value and  $\Omega_m h^2$  is varying. In (d)  $\Omega_b/\Omega_m$  is fixed and  $\Omega_m h^2$  is varying. In (b), (c) and (d)  $\Omega_m = 1$ . In all cases varying the parameter changes the pattern of Doppler peaks.

This figure "fig1-1.png" is available in "png" format from:

<http://arxiv.org/ps/astro-ph/9406050v1>

This figure "fig1-2.png" is available in "png" format from:

<http://arxiv.org/ps/astro-ph/9406050v1>